CHIANTI Paper XVIII – Advanced models for higher density plasma

Roger Dufresne[1], Giulio Del Zanna[1], Peter Young[2,3], Ken Dere[4],
Eva Deliporanidou[1], Will Barnes[2,5], Enrico Landi[6]

[1]University of Cambridge, [2]NASA GSFC, [3]Northumbria University,
[4]George Mason University, [5]American University, [6]University of Michigan

(ApJ, 2024, in press - arXiv:2403.16922)

Abstract: Version 11 of the CHIANTI database and software package is presented. Advanced ionization equilibrium models have been added for low charge states of seven elements (C, N, O, Ne, Mg, Si and S), and represent a significant improvement especially when modelling the solar transition region. The models include the effects of higher electron density and charge transfer on ionization and recombination rates. As an illustration of the difference these models make, a synthetic spectrum is calculated for an electron pressure of 7x10^{15} cm^{-3} K and compared with an active region observation from HRTS. Increases are seen of factors of two to five in the predicted radiances of the strongest lines in the UV from Si IV, C IV, and N V, compared to the previous modelling using the coronal approximation. Much better agreement (within 20%) with the observations is found for the majority of the lines. The new atomic models better equip both those who are studying the transition region and those who are interpreting emission from higher density astrophysical and laboratory plasma. In addition to the advanced models, several ion datasets have been added or updated, and data for the radiative recombination energy loss rate have been updated.

Background

Since the first release of CHIANTI in 1997 (Dere et al 1997) the coronal approximation has been used throughout to model ion fractions. However, this is inadequate for the lower atmosphere. For instance, using the coronal approximation for emission in the transition region predicts line intensities from C IV, N V, O VI, Si IV and S VI to be factors of 2-10 below observations. These lines are all from Li- and Na-like ions and have been termed anomalous ions. The differences in the modelling required for the different solar regions are illustrated below.

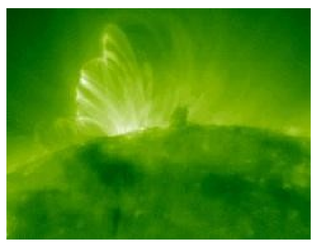

Corona (6x10^5-3x10^6 K) – steady state equilibrium, optically thin, independent atom models, ground level ionisation and recombination, electron collisions.

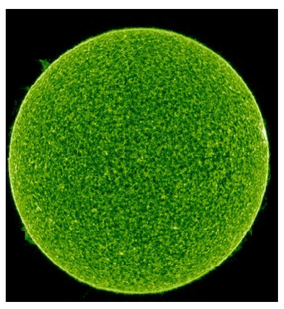

Transition region (25000-6x10^{5}K) – Generally steady state equilibrium but in some cases time dependent ionisation and radiative transfer included, density effects on free electron processes, charge transfer, photo-ionisation

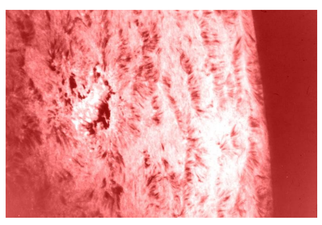

Chromosphere (6000-25000K) – Time-dependent ionisation, radiative transfer, photo-induced processes, charge transfer, inelastic collisions with hydrogen, (magneto-)hydrodynamics, partially-ionised plasma.

Recent atomic models

Dufresne and Del Zanna (2019) and Dufresne et al (2020,2021a,2021b) developed new atomic models for the lower solar atmosphere. They included all the atomic processes known to affect ion formation. Comparisons with quiet-Sun observations using differential emission measure (DEM) modelling showed improved agreements over and above the coronal approximation. Line intensities changed by factors of up to 7 for a number of lines (Dufresne et al 2023). Some of the greatest changes were to low temperature intercombination lines and lines from the anomalous ions.

The atomic models are included in CHIANTI to improve diagnostics for the transition region. The atomic data can also be used by those modelling the chromosphere.

Methods

The coronal approximation only includes ionisation and recombination from the ground states. Here ionisation and recombination is included for levels that become populated in the higher densities of the lower atmosphere, so-called metastable levels. Charge transfer, where an electron is exchanged during collisions with H and He, is also included in CHIANTI for the first time.

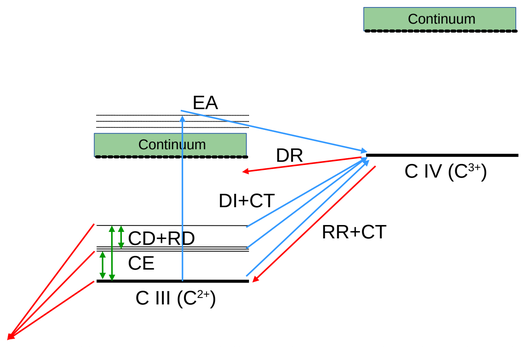

Figure 1. Schematic view of how ions are modelled in the advanced models. The included atomic processes are: DI – direct ionisation, EA – excitation-autoionisation, RR – radiative recombination, DR – dielectronic recombination, CE/CD – collisional excitation/de-excitation, RD – radiative decay, CT – charge transfer.

Ionisation rates are faster from the metastable levels than the ground; recombination rates are slower. This affects how the ions form. Ionisation rates were calculated for C and O, and estimated using Burgess and Chidichimo (1983) approximation for other elements. All recombination data is from the APAP network, www.apap-network.org (see Badnell et al 2003). Advanced models are available for: C, N, O, Ne, Mg, Si, S.

Results for the atomic modelling

1) Figure 2 shows that ion formation shifts to lower temperature for all ions compared to the coronal approximation. This changes the diagnostics of where ions form in the solar atmosphere.
2) Peak ion fractions increase for most ion stages. The peak ion fractions of Li- and Na-like ions (C IV, N V, O VI, Si IV) are substantially increased.
3) Line ratios will change using these models, including ratios of lines forming within the same ion.
4) Charge transfer primarily affects the ion balance between neutrals and singly-charged ions. However, all Si ions forming in the transition region are affected. Si IV forms over a much wider temperature range.

References

Dere, K. P., Landi, E., Mason, H. E., Monsignori Fossi, B. C., & Young, P. R. 1997, A&AS, 125, 149
Dufresne, R. P., & Del Zanna, G. 2019, A&A, 626, A123,
Dufresne, R. P., Del Zanna, G., & Badnell, N. R. 2020, MNRAS, 497, 1443
Dufresne, R. P., Del Zanna, G., & Badnell, N. R.. 2021a, MNRAS, 503, 1976
Dufresne, R. P., Del Zanna, G., & Storey, P. J. 2021b, MNRAS, 505, 3968
Dufresne, R. P., Del Zanna, G., & Mason, H. E. 2023, MNRAS, 521, 4696
Burgess, A., & Chidichimo, M. C. 1983, MNRAS, 203, 1269
Badnell, N. R., O'Mullane, M. G., Summers, H. P., et al. 2003, A&A, 406, 1151
Fontenla, J. M., Landi, E., Snow, M., & Woods, T. 2014, SoPh, 289, 515
Brekke, P. 1993, ApJS, 87, 443
Osborne C.M.J., Milic, I., 2021, ApJ, 917, 14
Asplund, M., Amarsi, A. M., & Grevesse, N. 2021, A&A, 653, A141

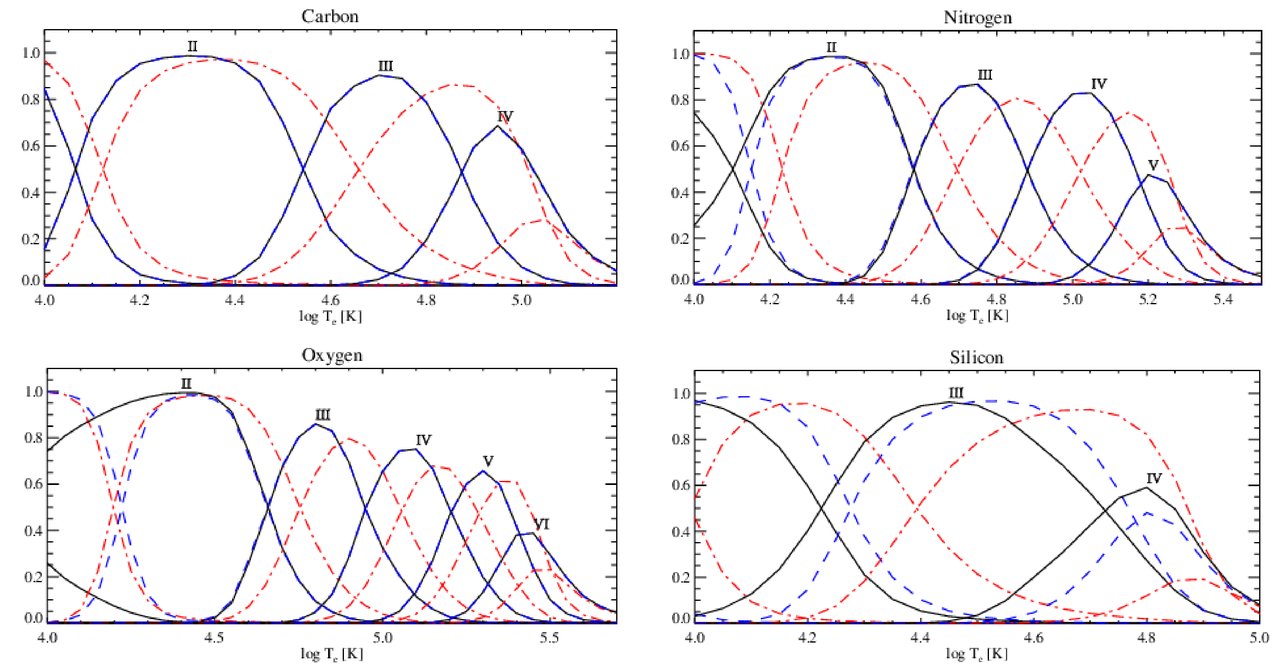

Figure 2. Fractional ion populations calculated with the present advanced models at a constant electron pressure of 7×10^{15} cm^{-3} K, with charge transfer included using the Fontenla et al. (2014) facula model atmosphere (black solid lines). Also shown are the advanced models without charge transfer (blue dashed lines) and the CHIANTI v.10.1 coronal approximation models (red dash-dotted lines).

Comparison with solar observations

The advanced models were used to calculate a synthetic spectrum using differential emission measure (DEM) modelling of an active region plage. Took observations from the High Resolution Telescope and Spectrograph (HRTS) on its second flight, as published by Brekke (1993). This had an absolute radiometric calibration and an uncertainty of 30%. It observed lines simultaneously in the wavelength range 1150-1600Å with a spectral resolution of 0.05Å. The density-sensitive 1399-1407Å O IV lines indicate a pressure of 7×10^{15} cm^{-3} K.

The 'CHIANTI_DEM' routine was run three times with everything the same except the ion fractions. Ion fractions were used from the advanced models with charge transfer, the advanced models without charge transfer, and the default CHIANTI ion fractions derived from the coronal approximation. The synthetic spectra are compared with the HRTS-II observations in Figure 3 below.

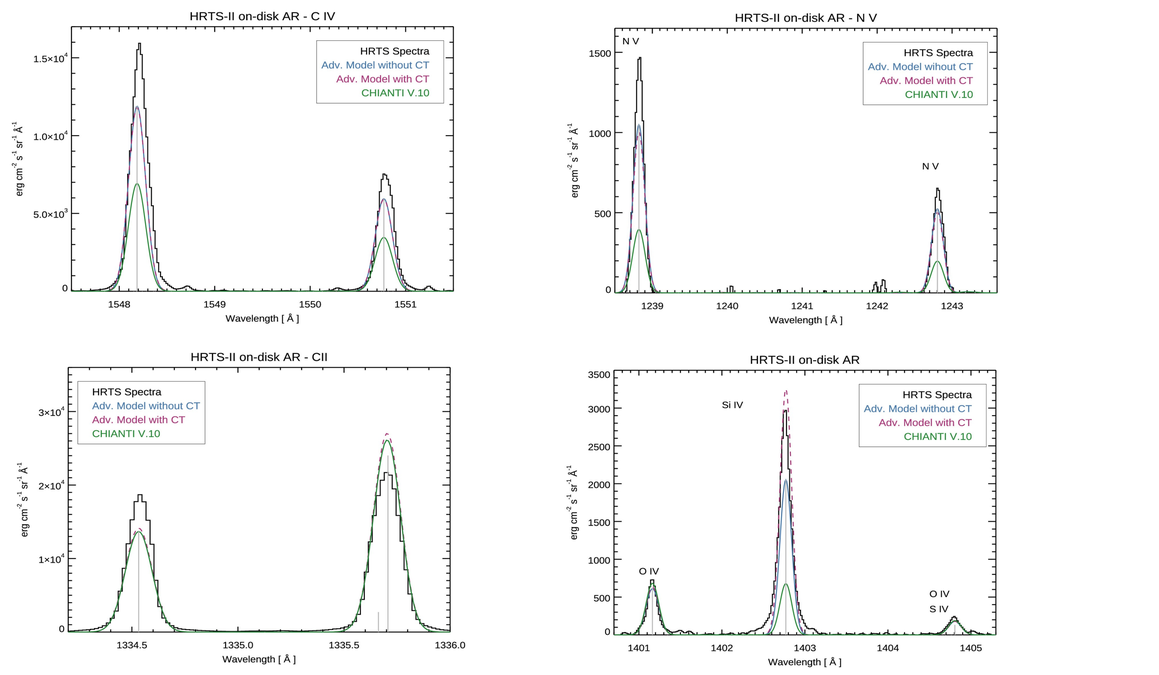

Figure 3. HRTS-II spectra (black lines) of an on-disk active region plage, superimposed with various synthetic spectra calculated using the present advanced models at a constant electron pressure of 7×10^{15} cm^{-3} K. Synthetic spectra obtained with the CHIANTI v.10.1 coronal approximation ion fractions are shown in green, the advanced model without charge transfer is shown in blue, and the advanced model with charge transfer is shown with a magenta dashed line. The theoretical wavelength for each transition is shown by a vertical grey line.

1) Enhancements of factors of 2 for C IV and N V line intensities and factor of 5 for Si IV lines intensities. They are in much better agreement with observations compared to the coronal approximation. Emission measure of these lines are now closer to other lines forming at a similar temperature. The results for all the lines used in the DEM modelling can be seen in Table 1.
2) Si IV and O IV lines observed by IRIS as well as O II and O VI lines observed by Solar Orbiter SPICE are all affected by the models.
3) Formation temperature of C II lines observed by IRIS is now 25,700K compared to 35,000K in coronal approximation. They form at even lower temperatures when photo-ionisation is included. The S IV lines observed by IRIS form at 66,000K instead of 89,000K
4) Element abundances of all lines, including Si and S, were well-represented by the photospheric abundances of Asplund et al (2021), indicating no FIP bias in this active region.

Table 1. Results of the DEM analysis of the HRTS-II plage. I_{obs} is the measured intensity in erg cm^{-2} s^{-1} sr^{-1}.

Wavelength (Å)	I_{obs}	Ion	Adv. models with CT		Adv. models without CT		CHIANTI v.10.1	
			log T_{eff}	I_{calc}/I_{obs}	log T_{eff}	I_{calc}/I_{obs}	log T_{eff}	I_{calc}/I_{obs}
1533.44	185	Si II	4.10	1.13	4.13	1.17	4.28	0.87
1264.74	276	Si II	4.15	0.70	4.18	0.79	4.40	0.82
1260.42	121	Si II	4.15	0.90	4.18	1.01	4.40	1.05
1259.52	67.2	S II	4.24	1.12	4.26	0.95	4.46	0.96
1253.81	53.0	S II	4.24	1.04	4.27	0.89	4.47	0.89
1250.58	37.4	S II	4.25	0.71	4.27	0.61	4.47	0.63
1194.45	134	Si II	4.26	1.06	4.28	1.22	4.46	1.38
1335.70	3450	C II	4.41	1.26	4.41	1.22	4.55	1.35
1334.53	2620	C II	4.41	0.85	4.42	0.82	4.56	0.93
1206.48	4920	Si III	4.55	0.83	4.59	0.90	4.64	0.82
1200.94	110	S III	4.60	0.97	4.61	1.00	4.69	0.82
1402.76	521	Si IV	4.73	1.10	4.78	0.70	4.91	0.23
1393.75	1500	Si IV	4.73	0.76	4.78	0.48	4.91	0.16
1247.39	16.7	C III	4.74	0.98	4.74	1.10	4.90	1.47
1423.84	5.15	S IV	4.82	1.07	4.81	1.17	4.95	0.96
1406.05	26.5	S IV	4.83	1.19	4.82	1.30	4.96	1.15
1550.79	1590	C IV	4.95	0.84	4.94	0.83	5.02	0.50
1548.21	3170	C IV	4.95	0.84	4.94	0.84	5.02	0.50
1486.51	31.4	N IV	5.02	0.93	5.02	0.93	5.08	0.96
1404.80	36.5	O IV	5.05	0.92	5.04	0.93	5.12	0.98
1407.38	26.9	O IV	5.07	1.28	5.08	1.24	5.12	1.34
1401.16	102	O IV	5.08	1.19	5.09	1.17	5.13	1.28
1199.17	46.9	S V	5.09	0.69	5.10	0.68	5.12	0.60
1238.82	240	N V	5.24	0.82	5.23	0.86	5.32	0.34
1218.35	203	O V	5.30	1.06	5.29	1.06	5.38	0.98

Conclusions

a) Advanced atomic models shift ion formation to lower temperatures and larger peak ion fractions, altering diagnostics for this region.
b) Enhanced emission from Li- and Na-like ions brings their emission measure into better agreement with neighbouring lines.
c) Charge transfer affects neutrals, singly-charged ions and all Si ions in the lower transition region.
d) The advanced models are switched on by default in CHIANTI, but charge transfer must be switched on using the keyword '/ct'. E.g. ch_synthetic,1390,1408,pressure=7.e15,/ct. Parameters from model atmospheres are included for calculating charge transfer rates.
e) Photo-ionisation is also important, especially for the lowest charge states. This and resonant photo-excitation are to be included in a future version of CHIANTI.
f) The effects of kappa electron distributions have been shown on the carbon advanced model in a new work (Dzifcakova et al 2024, A&A, accepted).
g) The data and models will be used for radiative transfer calculations using Lightweaver (Osborne and Milic 2021).
h) The new CHIANTI IDL models and atomic data are available from SolarSoft, the CHIANTI website (chiantidatabase.org), Github (github.com/chianti-atomic/chianti-idl) and CHIANTI-VIP (chianti-vip.com).